7.6. Barrow, Alaska

UV data from Barrow differ from the austral high latitude sites in several ways. For example, the "ozone-sensitive" data products, particularly biologically effective dose-rates and the integral around 300 nm, show much smaller short-term variability than at the austral sites due to less severe ozone depletion in the Arctic.

In Figure 7.6.1, recent column ozone data from the Ozone Monitoring Instrument (OMI) onboard NASA's AURA satellite are compared with ozone records from the years 1991-2011. There is a strong seasonal dependence: ozone columns are generally higher and have a larger variability during spring than autumn. Measurements in 2012 showed a particular large variability in February and March. Ozone values on 2/26/12 and 3/9/12 were amongst the highest values measured for these days. This is in stark contract to 2011 (see report from previous year), when total ozone across the Arctic was unprecedentedly low. Ozone values between April and October scattered about the long-term average (blue line) with two notable exceptions:

- Total ozone was 257 DU on 6/9/12 and 267 DU on 6/10/12. The long-term mean for the two days is 345 DU and the standard deviation of the year-to-year variability is 23 DU. Thus, total ozone on these two days was 3.8 and 3.4 standard deviations below the climatology. Satellite images (e.g., http://www.temis.nl/protocols/o3field/o3month_omi.php?Year=2012&Month=06&View=np) indicate that the low-ozone event was caused by advection of ozone-poor air from lower latitudes originating from above the United States. The transport of ozone-poor air from lower to higher latitudes is well documented, but advection from sub-tropical to polar latitudes is less common. As a consequence of low ozone, the UV Index at Barrow on 6/10/12 was 40% above the mean value for this day (Figure 7.6.2).
- Total ozone on 9/27/12 was 366 DU, which is about 65 DU larger than the long-term mean for this day. The standard deviation of the year-to-year variability is 28 DU.

The low-ozone event of June led to unusually high UV intensities in many data products. For example, spectral irradiance integrated over 298.51 - 303.03 nm (Figure 7.6.3) showed new record values.

Figure 7.6.4 and Figure 7.6.5 show the annual cycles of DNA- and erythemally-weighted daily dose, respectively. Daily irradiation in the 400-600 nm band is shown in Figure 7.6.6. Visible radiation is much more affected by clouds during summer and autumn than during spring.

Factors affecting the annual cycles in UV and visible radiation at Barrow have been analyzed in great detail (*Bernhard et al.*, 2007). The annual ozone cycle was found to be the dominant parameter modifying UV-B irradiance, but the combined effects of albedo and clouds compensate for most of the ozone influence. High surface albedo caused by snow cover may increase UV irradiance by up to 57%. Aerosols lead to reductions of 5% typically, but larger reduction was observed during Arctic haze events, particularly during spring. For erythemal irradiance, and measurements in the UV-A and visible, annual cycles of albedo and clouds are responsible for a pronounced seasonal asymmetry.

An example of the different characteristics of DNA-damaging and visible radiation is shown in Figure 7.6.7. Daily irradiation in the 400-600 nm spectral range is not centered at the summer solstice but shifted by about 15 days towards spring. The DNA curve on the other hand is nearly symmetrical with respect to the solstice. The reason for this distinct difference can be explained as follows: surface albedo is larger and clouds are less prevalent in spring than in autumn. This enhances radiation levels in spring and is the reason of the apparent shift of measurements in the visible. Higher albedo and less cloudiness also leads to larger DNA-damaging radiation, but the larger total ozone column in spring (Figure 7.6.1) compensates the enhancement. As a consequence, DNA-damaging radiation is of similar magnitude in spring and autumn.

Reference:

Bernhard, G., C. R. Booth, J. C. Ehramjian, R. Stone, and E. G. Dutton (2007), Ultraviolet and visible radiation at Barrow, Alaska: Climatology and influencing factors on the basis of version 2 National Science Foundation network data, J. Geophys. Res., 112, D09101, doi:10.1029/2006JD007865.

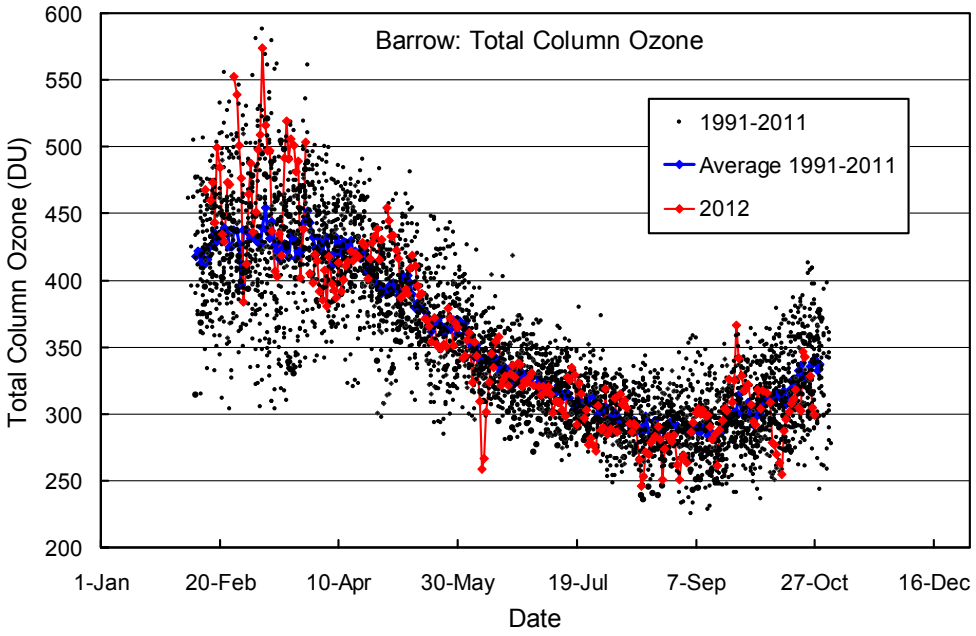

Figure 7.6.1. *Total column ozone at Barrow. OMI measurements from 2012 are contrasted with ozone data from prior years recorded by TOMS on Nimbus-7 (1991-1993), Earth Probe (1996-2004), and OMI (2005-2011) satellites. TOMS data are from the Version 8 data set.*

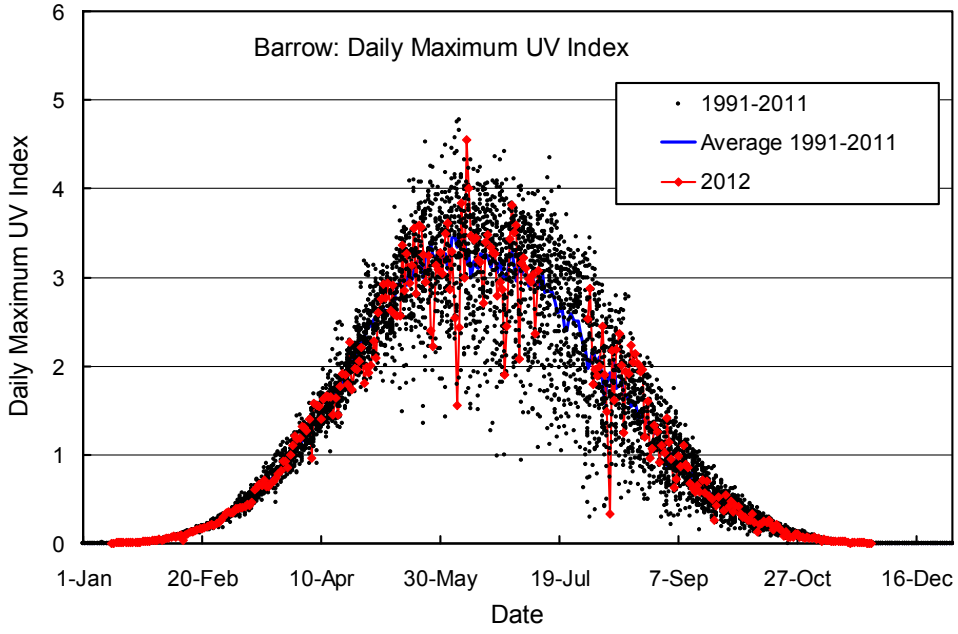

Figure 7.6.2. *Daily maximum UV Index at Barrow. Measurements from 2012 are contrasted with individual data points and the average of measurements taken between 1991 and 2011.*

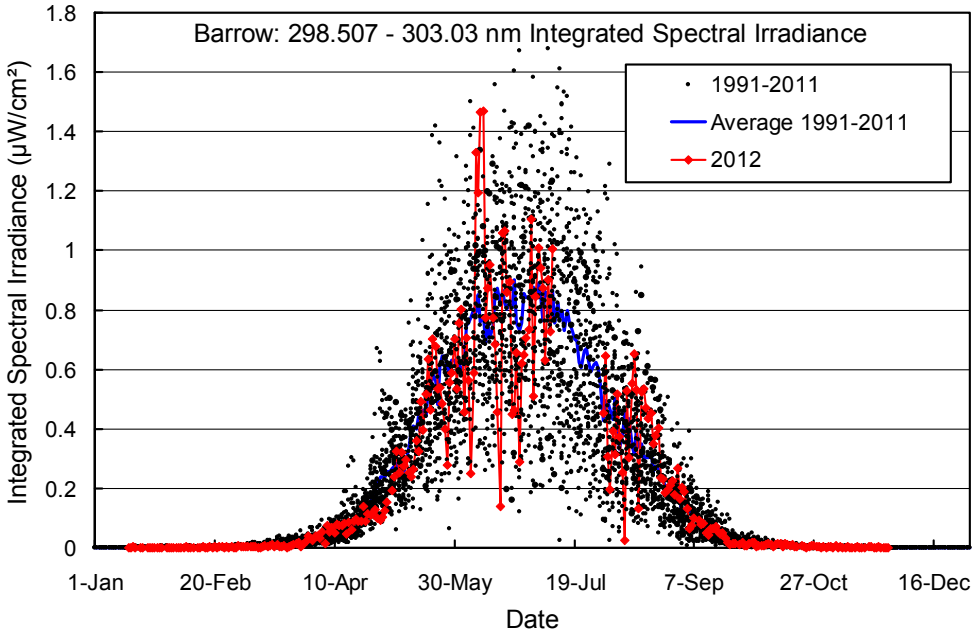

Figure 7.6.3. *Noontime integrated spectral UV irradiance (298.51 - 303.03 nm) at Barrow. Measurements from 2012 are contrasted with individual data points and the average of measurements taken between 1991 and 2011.*

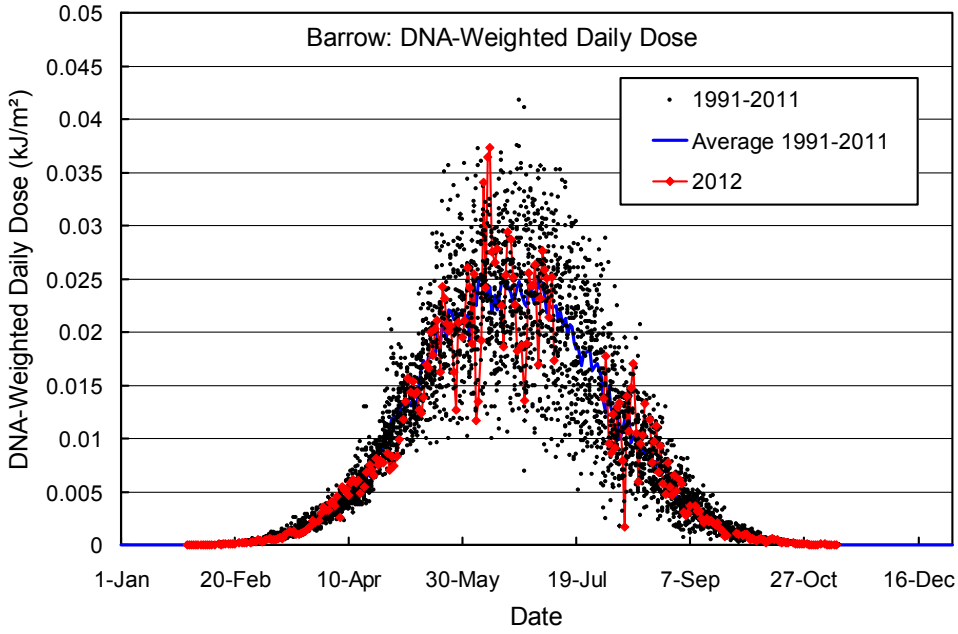

Figure 7.6.4. *Daily DNA-weighted dose at Barrow. Volume 22 measurements from 2012 are contrasted with individual data points and the average of measurements taken between 1991 and 2011.*

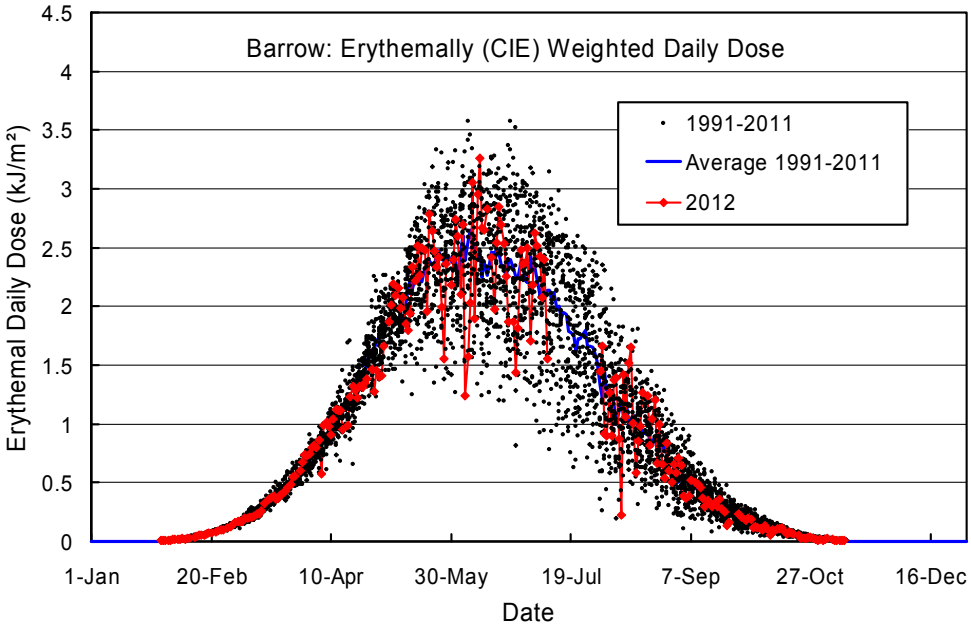

Figure 7.6.5. *Daily erythemal dose at Barrow. Volume 22 measurements from 2012 are contrasted with individual data points and the average of measurements taken between 1991 and 2011.*

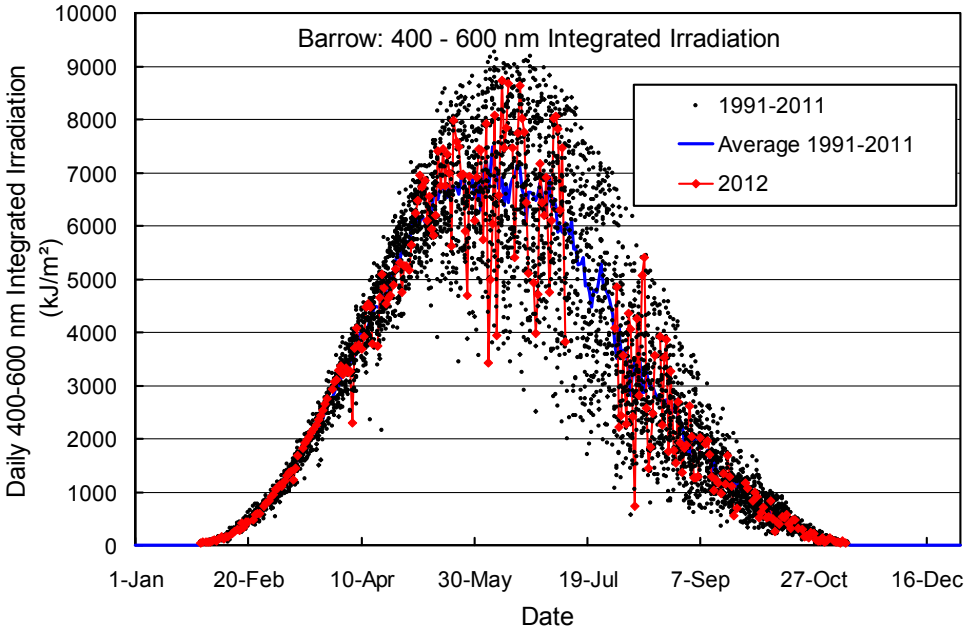

Figure 7.6.6. *Daily irradiation of the 400-600 nm band at Barrow. Volume 22 measurements from 2012 are contrasted with individual data points and the average of measurements taken between 1991 and 2011.*

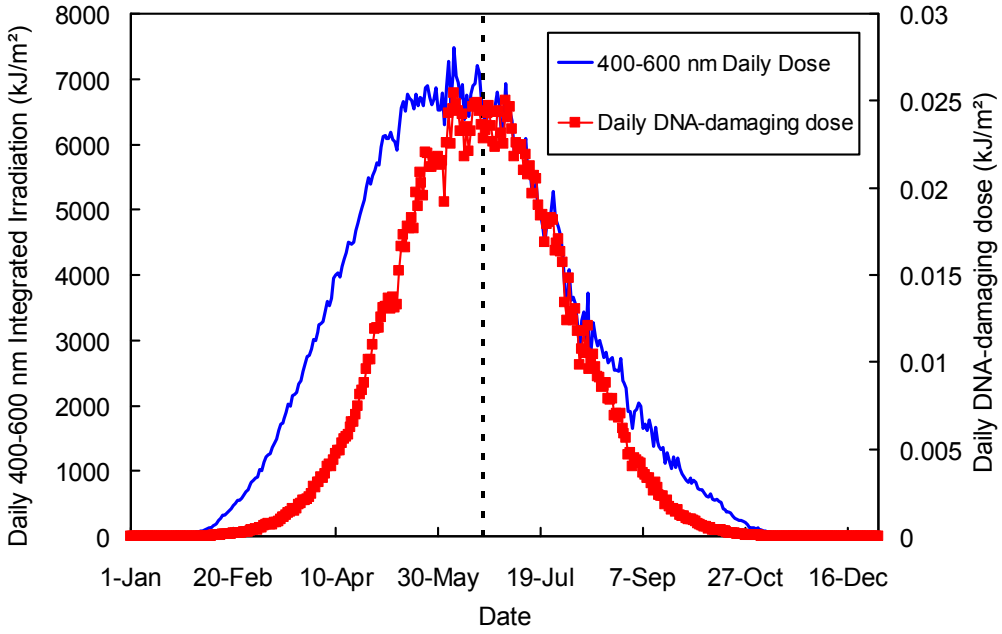

Figure 7.6.7. *Comparison of DNA-weighted dose (right axis) with daily irradiation in the 400-600 nm spectral range (left axis) at Barrow. Both curves are average values for the period 1991-2011.*